Analogue wavelet transform with single biquad stage per scale

M.A. Gurrola-Navarro and G. Espinosa-Flores-Verdad

A new approach to obtain the wavelet transform with easily constructed analogue circuits is presented. It is shown that the impulse response of a bandpass biquad filter satisfies the conditions to be considered a mother wavelet. Using this, an integrated circuit performing the wavelet transform at 16 scales along eight octaves has been designed. The design has CMOS transistors working in the subthreshold region with a total power consumption of 650 nW. On-chip measurements are reported.

Introduction: Traditionally, the wavelet transform (WT) is implemented numerically or algorithmically. Recently, there have been significant advances in the analogue implementations of this transform and its practical applications [1, 2]. The analogue realisation is attractive for low power signal processing in areas such as portable and bio-implantable devices. Currently, the common analogue approach is to obtain each scale of the WT by means of convolution in a bandpass continuous filter, the impulse response of which has the wavelet shape. References [1, 2] have applied this principle with favourable results. These works show efforts to obtain good approximations of the known classical wavelets: the Morlet wavelet [1], and the first derivative of a Gaussian [2]. However, to obtain a good approximation, the filters have to be of high order, since the shape of classical wavelets is not the natural impulse response of the simpler analogue filters. In this Letter, we show that the impulse response of a bandpass biquad filter is a mother wavelet.

Wavelet transform review: Beginning with a function $\psi(t)$, referred to as the mother or prototype wavelet, we obtain

$$\psi_{r^m}(t) = (1/r^m)\psi(t/r^m) \tag{1}$$

which is a family of functions scaled by a factor of r^m, for an arbitrary number $r > 1$, where m is an integer. Now, we define the direct WT by

$$W_{r^m}f(b) = \int_{-\infty}^{\infty} f(t)\psi_{r^m}(t-b)dt \tag{2}$$

where $f(t)$ is the input signal, and $W_{r^m}f(b)$ is the WT component at the mth scale. This kind of WT (discrete in scale and continuous with respect to time translation) is called semidiscrete WT, or dyadic WT for the particular case when $r = 2$ [3]. Note that $W_{r^m}f(b)$ is the convolution between $f(t)$ and $\psi_{r^m}(-t)$. This convolution can be achieved using a continuous filter with an impulse response equal to $\psi_{r^m}(-t)$.

To obtain the mother wavelet, we use the filter

$$H(\omega) = \frac{(\omega_o/q)j\omega}{(j\omega)^2 + (\omega_o/q)j\omega + \omega_o^2} \tag{3}$$

with $q = \sqrt{2}$, $\omega_o = 2\pi f_o, f_o = 13.45$ kHz. The impulse response of this filter, hereafter referred to as $h(t)$, is shown in Fig. 1*a*. As is stated in (1), the mother wavelet $\psi(t) = h(-t)$ has to be scaled to obtain $\psi_{r^m}(t) = h_{r^m}(-t) = (1/r^m)h(-t/r^m)$. In the frequency domain, it implies that $H_{r^m}(\omega) = H(r^m\omega) = \Psi^*(r^m\omega)$, where $\Psi^*(\omega)$ is the Fourier transform of $\psi(t)$, and the asterisk (*) stands for complex conjugation. Note that if ω_o and ω_m are the central frequencies of $H(\omega)$ and $H_{r^m}(\omega)$, respectively, then

$$\omega_m = \omega_o/r^m \tag{4}$$

In the following Sections, we prove that $\psi(t) = h(-t)$ satisfies the admissibility and the stability conditions of the semidiscrete WT, as is required to be considered a prototype wavelet.

Admissibility proof: For the admissibility condition, it is required that [3]

$$C_\psi = 2\int_0^{\infty} |H(\omega)|^2/\omega\, d\omega < \infty \tag{5}$$

Splitting this integral we have

$$C_\psi = 2\int_0^{\omega_o} |H(\omega)|^2/\omega\, d\omega + 2\int_{\omega_o}^{\infty} |H(\omega)|^2/\omega\, d\omega \tag{6}$$

where $H(\omega)$ is given by (3). In the Bode plot of Fig. 1*b*, it can be seen that the integrand $|H(\omega)|^2/\omega$ is bounded, and the first integral must be bounded. Hence, the convergence of C_ψ depends on the convergence of the second (improper) integral. In the same Bode plot, it can be seen that the curve of the integrand is always bellow the function $10^{11}/\omega^3$. Therefore, the original improper integral converges because $\int_{\omega_o}^{\infty} 10^{11}/\omega^3\, d\omega$ converges.

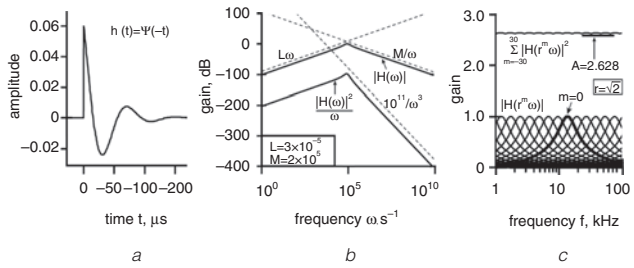

Fig. 1 *Proposed wavelet and auxiliary figures*

a Prototype wavelet
b Bode plot of functions $|H(\omega)|^2/\omega^3$ and $|H(\omega)|$
c Several functions $|H(r^m\omega)|$, and summation $\sum_{m=-30}^{30}|H(r^m m)|^2$

Stability proof: For the stability condition of the semidiscrete WT [3], constants A and B are required such that, for $0 < \omega < \infty$,

$$0 < A \le \sum_{m=-\infty}^{\infty} |H(r^m\omega)|^2 \le B < \infty \tag{7}$$

For this research, we selected $r = \sqrt{2}$, meaning that the WT system will have two scales per octave. (The number of scales per octave of frequency in the system is given by $(\log_2 r)^{-1}$.) Fig. 1*c* shows several spectra $|H(r^m\omega)|$, and summation $\sum_{m=-30}^{30} |H(r^m\omega)|^2$. This summation shows its periodical behaviour when it is plotted on a logarithmic ω-axis. We have numerically found that this ripple has a minimum value of $A = 2.628$. Note that using $-30 < m < 30$ is a sufficient approximation to find a lower bound A required by (7) since it is a summation of non-negative terms. On the other hand, in the Bode plot of Fig. 1*b*, it can be seen that $|H(\omega)|$ is always below the curves of $L\omega$ and M/ω, where $L = 3 \times 10^{-5}$ and $M = 2 \times 10^5$. Considering that $L\omega$ and M/ω are increasing and decreasing monotonic functions, respectively, we have that

$$|H(\omega)| \le L\omega_x \quad \text{for} \quad \omega \in [r^{-1}\omega, \omega] \tag{8}$$

$$|H(\omega)| \le M/\omega_x \quad \text{for} \quad \omega \in [\omega, r\omega] \tag{9}$$

Now, we develop the summation in (8) to find the required upper bound B:

$$\begin{aligned}\sum_{m=-\infty}^{\infty} |H(r^m\omega)|^2 &\le \sum_{m=-\infty}^{0} (Lr^m\omega_l) + \sum_{m=0}^{\infty} (M/r^m\omega_l)^2 \\ &= (L^2\omega_l^2 + M^2/\omega_l^2)r^2/(r^2-1) = B\end{aligned} \tag{10}$$

where ω_l is any desired frequency in the range $(0,\infty)$. Taking $\omega_l = \omega_o$ (3), we obtain $B = 442.55$, for the given r.

Circuit implementation: For circuit implementation we restrict the scales to the values $m = 0,1, \ldots,15$, resulting in a system with a total of 16 filters working through eight octaves in the audiofrequency range. The circuit in Fig. 2*a* has been used for the implementation of the system. It is composed of 16 identical Gm-C biquadratic filters and a voltage adder. The operational transconductance amplifier (OTA) used is shown in Fig. 2*b*, and has a range of ± 29.2 mA of linearity within 1% of distortion [4]. The wavelet components are represented by the signals v_k (for $k = 0, 1, \ldots,15$), with the transfer function

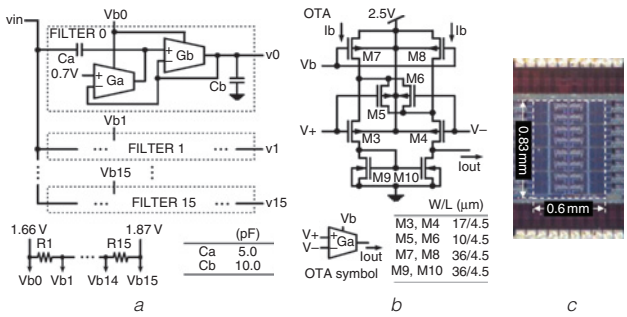

Fig. 2 *Circuit and manufactured chip*

a Biquad filter and resistor ladder
b Operational transconductance amplifier (OTA)
c Microphotograph of system in manufactured chip

$$\frac{V_k(s)}{V_{in}(s)} = \frac{(\omega_k/q)s}{s^2 + (\omega_k/q)s + \omega_k^2} \tag{11}$$

where $q = \sqrt{C_b/C_a} = \sqrt{2}$, and $\omega_k = G/\sqrt{C_a C_b}$ (with $G = G_a = G_b$). This function has the same structure required by (3).

The OTAs are biased in the subthreshold region. In this case, the nominal transconductance is given by $G = I_b\rho/3V_t$, where $\rho \simeq 0.7$ is the electrostatic coupling between gate and channel, and V_t is the thermal voltage [4]. Additionally, the bias current is given by $I_b \propto \exp(\rho(2.5 - V_b)/V_t)$ [5]. Therefore, G (and ω_k) has exponential dependence with respect to nearly linear changes in V_b. The circuit also includes a ladder of 15 resistors of nearly equal value (R_1 to R_{15}) biased by the external voltages 1.66 and 1.87 V. The resulting nearly equispaced bias voltages (V_{b0} to V_{b15}) produce exponentially spaced values for ω_k, as required by (4).

Experimental results: A chip with the designed system (Fig. 2*c*) has been fabricated in a 0.5 μm CMOS technology. The system covers an area of about 0.50 mm^2, with power consumption of 650 nW. The noise level was measured at 0.6 mV of standard deviation at any output of the system. To reduce the noise level, and achieve a better understanding of the transform capabilities of the system, the probe signal shown in Fig. 3*a* has been periodically applied in the circuit. Each output has been averaged over 128 periodical samples using a digital oscilloscope. The probe signal is composed of three sinusoidal pulses of 2 kHz, 1 kHz, and 500 Hz, where the envelope function is a half sinusoidal wave of 50, 25, and 12.5 kHz, respectively.

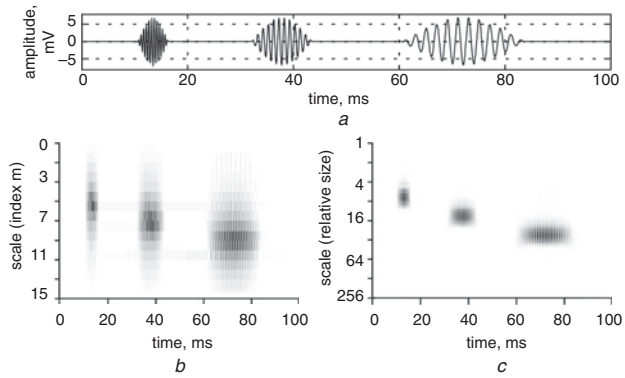

Fig. 3 *Experimental results*

a Probe signal
b Analogue WT measured at 16 outputs (v_0 to v_{16}) of chip
c Continuous WT numerically obtained for comparison

The absolute values of the AC components of the on-chip measured signals (v_0 to v_{15}) have been plotted as an image in Fig. 3*b*. For comparison, Fig. 3*c* shows the numerical continuous WT of the same probe signal with respect to the Morlet wavelet. Note that the chip actually performs the WT of the probe signal reflecting the higher frequencies at lower scales and the low frequencies at higher scales. As can be seen, the continuous (numerical) WT has better time-frequency resolution (the shadow area of the transform is more concentrated). This is because the minimum possible time-frequency resolution is obtained using the Morlet wavelet. We expect that using biquad filters with greater selectivity the resolution in frequency (scale) will increase, but at the expense of a minimal loss in the resolution in time.

Conclusion: We have shown that the impulse response of the bandpass biquad filter is a mother wavelet. As a consequence, we have an alternative to construct analogue WT systems with very few components. The proposed system has been fabricated in CMOS technology with power consumption of 650 nW. The shown approach can be applied to bandpass filters with different selectivity or of higher order.

Acknowledgment: M. Gurrola-Navarro thanks the Mexican Council of Science and Technology (CONACYT) for his doctoral scholarship.

14 February 2010
doi: 10.1049/el.2010.0437
One or more of the Figures in this Letter are available in colour online.

M.A. Gurrola-Navarro (*Dpto. de Electrónica, CUCEI, Universidad de Guadalajara, Av. Revolución 1500, Guadalajara, Jal., CP 44430, México*)

E-mail: marco.gurrola@cucei.udg.mx

G. Espinosa-Flores-Verdad (*Dpto. de Electrónica, Instituto Nacional de Astrofísica Óptica y Electrónica, Luis Enrique Erro 1, Tonantzintla, Pue., CP 72840, México*)

References

1 Haddad, S.A.P., Bagga, S., and Serdijn, W.A.: 'Log-domain wavelet bases', *IEEE Trans. Circuits Syst. I*, 2005, **52**, (10), pp. 2023–2032
2 Hongmin, L., Yigang, H., and Sun, Y.: 'Detection of cardiac signal characteristic point using log-domain wavelet transform circuits', *Circuits Syst. Signal Process.*, 2008, **27**, (5), pp. 683–698
3 Chui, C.K.: 'Wavelet analysis and its applications: Volume 1: An introduction to wavelets' (Hartcourt Publishers, San Diego, CA, USA, 1992)
4 Furth, P.M., and Andreou, A.G.: 'Cochlear models implemented with linearized transconductors'. Proc. IEEE, Int. Symp. Circ. and Syst., Atlanta, GA, USA, 1996, Vol. 3, pp. 491–494
5 Watts, L., Kerns, D.A., Lyon, R.F., and Mead, C.A.: 'Improved implementation of the silicon cochlea', *IEEE J. Solid-State Circuits*, 1992, **27**, (5), pp. 692–700